

# A STUDY OF THE RELATIVE RATES OF METEORITE FALLS ON THE EARTH'S SURFACE

**Ian Halliday and Arthur A. Griffin**

*Herzberg Institute of Astrophysics  
National Research Council of Canada  
Ottawa, Canada K1A 0R6*

*Meteorite camera networks have provided reliable data on typical orbits for meteorites. Using an adopted distribution of 20 orbits we determine the relative rates of meteorite falls over the surface of the earth taking account of the important effects due to the earth's gravity. The data are then used to study the expected variation in rates as a function of daylight, twilight or night conditions; time of day; season of the year; and geographic latitude.*

*The rates of meteorite falls have a deep minimum near the area of the earth facing the earth's apex but a surprisingly broad maximum on the opposite side, facing the antapex. Twilight rates are lower than average and nighttime rates 3% higher than daytime rates. Minimum rates occur near 6<sup>h</sup> local time and there is a broad maximum from noon to midnight. Rates are highest near the beginning of spring for either hemisphere and lowest near the beginning of autumn. The decline in rates with increasing latitude is quite moderate. The existing camera networks observe average fall rates at night which are very close to the average rate over the whole earth for the whole year.*

## INTRODUCTION

Studies of the statistics of meteorite falls may be severely biased by numerous factors. Among the important factors are: (1) *the type of meteorite*, which greatly affects the probability of recognition of the meteorite for finds and even for falls when the actual impact on the ground was not witnessed; (2) *the time of day*, since the chance of observing the fireball may be better in darkness but the chance of observing the impact is not only greater during daylight but social factors may also produce large variations in the potential audience available to witness the event; (3) *the time of year*, since the probability of recovery will vary with wet, dry, frozen or snow-covered ground and the social factors again come into play; (4) *the geographic latitude of the event*, which may be relatively favorable or unfavorable for the arrival of a meteorite in a particular orbit.

Attempts may be made to determine empirical correction factors for some of the effects mentioned above, but the assumptions which must be made are likely to render the conclusions unconvincing. The fireball camera networks appear to be in a position to avoid the social biases but their observations are restricted to the hours of darkness and the data from one network refer to an essentially constant latitude. With recent progress in the identification of those fireballs which are associated with meteorites, it does appear that data from the networks can be used for the statistical problem. This approach may be expected to yield results which are superior to those based on the incomplete data from meteorite recoveries.

The Canadian camera network is known as the Meteorite Observation and Recovery Project (MORP) and its design and operation have been described previously (Halliday, 1973; Halliday *et al.*, 1978). One of the aims of the project is to determine the flux of

meteorite arrivals and, for this purpose, a large effort is expended in maintaining records of the area of the atmosphere and the number of clear-sky hours suitably observed by the network. The observations are made only during darkness near a mid-latitude for the network of 52° N. One purpose of this paper is to investigate how the flux of meteorites observed under these conditions is expected to differ from the average flux for the whole earth.

The crucial assumption, which replaces the assumptions mentioned in the second paragraph, is the following: as a result of nearly two decades of observations by camera networks, we can specify a distribution of orbits which adequately represents the distribution of orbits among those meteoroids which produce meteorites. Each representative member of the adopted distribution can be studied for the pattern of its probable collisions with the earth. The sum of all such patterns is then used to derive the diurnal and annual variations for any chosen geographic location.

### SELECTION OF METEORITE ORBITS

Wood (1961) used a nineteenth century compilation of meteorite radiants to show that the distribution was incompatible with a lunar origin but agreed satisfactorily with an asteroidal source for stone meteorites. Millman (1969) examined the observations of the fireballs associated with 25 meteorites and derived a set of orbits for each event, corresponding to different assumed velocities combined with the observed radiant. Simonenko (1975) studied the variation in orbital elements of 45 meteorites if the apparent radiant was considered to have an uncertainty of up to 10° in its position. For each radiant she used four values for the atmospheric entry velocity, ranging from 13 to 22 km s<sup>-1</sup>. Both studies indicate that typical meteorite orbits are direct orbits of low inclination with aphelia in the asteroid belt.

The earth's atmosphere acts as a filter which discriminates against the survival of meteorites from meteoroids with high geocentric velocity. Levin and Simonenko (1969) adopted 22 km s<sup>-1</sup> as the upper limit for survival, which was an upward revision of Levin's previous limit of 20 km s<sup>-1</sup>, to allow for the fact that Pribram, the only well observed meteorite fall at that time, had a geocentric velocity of 20.9 km s<sup>-1</sup>. ReVelle's (1979) theory of meteorite entry indicates an upper limit between 25 km s<sup>-1</sup> and 30 km s<sup>-1</sup> for survival of some material from chondrites.

We wish to adopt a distribution of orbits to represent the population of meteorites arriving at the earth. Since there are only three meteorites with secure orbital elements from the camera networks, we augment this sample by adding fireballs for which a study of the trajectory has indicated the material was probably similar to ordinary chondrites. The data come from three sources: (1) the group I fireballs in the study of Prairie Network data by Ceplecha and McCrosky (1976) based on their PE criterion; (2) the group I fireballs, based on the same criterion, in a list of 42 fireballs observed in central Europe (Ceplecha, 1977); (3) a group of 9 fireballs observed by the MORP network for which we believe a meteorite of at least 100 grams in mass reached the ground. Each source contributes one of the photographed meteorites, respectively Lost City from the Prairie Network, Pribram from the European data and Innisfree from the MORP network.

The first two lists include fireballs presumed to be produced by typical meteorite classes but which arrive with too high a velocity to expect a meteorite to survive the atmospheric filter. We discard all fireballs with an observed velocity greater than 25 km s<sup>-1</sup>, which reduces the total group from 115 to 74 fireballs. The effect of this selection is

to remove most objects with a perihelion distance less than 0.6 AU, especially if they also have inclinations in excess of about  $25^\circ$ .

To keep the amount of calculation within reasonable limits we represent the population of 74 fireballs by 20 hypothetical orbits which were selected so that plots of  $a$  vs.  $q$ ,  $a$  vs.  $i$ , and  $q$  vs.  $i$  are similar to the corresponding plots for the 74 fireballs ( $a$  = semi-major axis,  $q$  = perihelion distance,  $i$  = inclination of the orbit). The 20 values of  $a$ ,  $q$ ,  $i$  are shown in Table 1 which is arranged in order of increasing semi-major axis. Since the individual distributions of elements are not symmetrical, the median values may be more meaningful than the arithmetic means. The median values are:  $a = 2.08$  AU,  $q = 0.88$  AU,  $i = 6^\circ$ .

The question arises as to whether any group of meteorite orbits is excluded because the observational data from the camera networks were all collected at night. There is no such danger, as can be seen from plots of the orbital elements, where the only exclusions are those combinations which produce high geocentric velocities. There are no Aten-type fireballs ( $a < 1.0$  AU) in the group of 20 typical orbits since the entire group of fireballs contained only one orbit of this type. Such objects do not arrive preferentially during the day in any case.

## STATISTICAL ANALYSIS

The analysis involving the assumed distribution of orbits to derive the expected distribution of meteorite falls over the earth as a function of time and position requires several steps. For each of the 20 orbits, the pattern is derived of the relative intensity of bombardment on the earth's surface as a function of distance from the central point of the approximately hemispherical area within which meteorite falls may occur (the point for which the radiant is in the zenith). Each assumed orbit can encounter the earth in four different orientations (described below) with respect to the earth's orbital motion. By combining the contributions of all 80 cases, relative values of the instantaneous rates of meteorite falls are obtained for the earth's surface using a coordinate system based on the ecliptic pole, the direction to the apex of the earth's motion and the anti-solar direction. Since the real earth rotates and its axis describes an annual circle in the coordinate system just described, it is necessary to follow the motion of any chosen location in the system, i.e. construct tables or curves as a function of geographic latitude, time of day and time of year. From these tables one may derive the relative rates of meteorite falls for any comparison which is of interest.

To simplify the calculations it is essential to make certain assumptions, to which we draw attention. It is assumed that: (1) the earth's orbit is a circle of radius 1 AU; (2) the inclination of the ecliptic to the invariable plane of the solar system, estimated as  $1.6^\circ$  (Misconi, 1980) may be neglected; (3) there are no preferential longitudes for the nodes of the meteoroid orbits, hence the contribution from each of the 20 orbits over the whole earth does not depend on the time of year; (4) the effect of the earth's rotation on the observed velocity of a fireball (diurnal aberration) may be neglected relative to the geocentric velocity.

### *Detailed calculations*

For any assumed meteorite orbit, consider a stream of meteoroids moving in parallel paths along such an orbit, all approaching the vicinity of the earth. The earth's gravitational field increases the velocity of arrival and changes the direction of arrival (zenith attraction).

The effects are appreciable only within a few tens of earth radii of the earth but at the relatively low velocities which are typical of meteorites, the gravitational focusing is quite considerable. This part of the problem was treated in an earlier paper (Halliday, 1964) which dealt with one aspect of the present paper using a more restrictive assumption about orbital inclinations.

From a standard treatment of planetary orbits (see, for example, van de Kamp, 1960, chapter III) one can use the assumed orbital elements of Table 1 to determine the heliocentric velocity of the meteorite at 1 AU and also the geocentric velocity without the earth's gravitational influence,  $V_G$ . For each entry in Table 1, the equation for the orbital motion of the meteorite about the earth was used to compute the impact point for an object deflected by the earth's gravity from an initial distance of 40 earth radii. The impact point is described by the angle  $\theta$  between the point of impact and the central point (at which the radiant is in the zenith). Eleven initial displacements from the center of the hypothetical beam of meteoroids were chosen, defining eleven concentric zones, the first two containing 0.01, 0.09, and nine further zones each with 0.1 of the total flux. The values of  $\theta$  determine the target rings on the earth's surface over which the meteorites from each zone are distributed, hence the relative values of the rates per unit area may be plotted as a function of  $\theta$ . The rates are normalized to give an average value of 1.0 over the entire sphere for each entry in the table.

Figure 1 shows three of these curves for different values of  $V_G$ . The maximum values of  $\theta$  define the total area over which meteorites with the particular orbit could land, ranging from  $121^{\circ}02$  for the slowest member to  $\theta = 97^{\circ}83$  for the largest value of  $V_G$ . Table 1 shows the values of  $V_G$  and also the values of  $V_{\infty}$ , the velocity of arrival at the earth, which corresponds to the observed velocity at the upper limit of the photographic trail except for the minor effect of diurnal aberration.

A cubic equation of the form:

$$R = a + b\theta^2 + c\theta^3 \quad (1)$$

fits the curves of Figure 1 very well, with individual values of the constants for each of the 20 curves. For meteor number 1 the coefficients are:  $a = 3.167$ ,  $b = -4.192 \times 10^{-4}$ ,  $c = 1.199 \times 10^{-6}$  with  $\theta$  expressed in degrees.

For each of these meteors there are four geometrical orientations for the earth-meteor encounter; with the meteoroid approaching perihelion at the descending node or at the ascending node, plus the post-perihelion case at the two nodes. The four paths all make the same angle with the apex-antapex line but the first two cases will tend to be night events and the other two will have a correspondingly high proportion of daytime encounters.

To evaluate the relative fluxes over the earth we again choose a coordinate system defined by the anti-solar direction, the earth's apex and the ecliptic pole and divide the earth's surface into many small cells of equal area. We chose  $6^{\circ} \times 6^{\circ}$  for each cell and divided the sphere into strips each  $6^{\circ}$  in width, beginning from the sunrise-sunset line and proceeding toward the sub-solar and anti-solar points. Each hemisphere was thus divided into 573 cells and the choice of the terminator as the reference circle has the benefit of defining the twilight zone (nautical twilight or brighter) as the first two bands, consisting of 60 and 59 cells respectively. The 20 meteor orbits produce 80 directions for the radiant as we have seen, and for each of these 80 cases the contribution in each of the 1146 cells was computed from the appropriate version of equation (1). Negative values for R are not

**Table 1**  
Assumed distribution for 20 typical meteorite orbits

No.	a	q	i	$V_G$	$V_z$
1	1.30	.770	16	14.26	18.08
2	1.45	.650	6	16.66	20.03
3	1.56	.850	2	10.99	15.63
4	1.60	.700	5	16.08	19.55
5	1.64	.990	9	7.75	13.56
6	1.70	.620	2	18.82	21.86
7	1.78	.970	8	8.70	14.12
8	1.89	.750	3	15.78	19.31
9	1.96	.995	18	12.35	16.62
10	2.04	.900	1	11.19	15.78
11	2.12	.660	10	19.96	22.85
12	2.18	.985	1	7.99	13.69
13	2.22	.930	19	15.08	18.74
14	2.24	.740	11	18.15	21.29
15	2.30	.950	5	10.27	15.14
16	2.48	.980	3	9.04	14.33
17	2.50	.770	10	17.67	20.88
18	2.54	.860	20	17.87	21.04
19	2.60	.940	6	11.42	15.94
20	3.20	.950	3	11.42	15.94

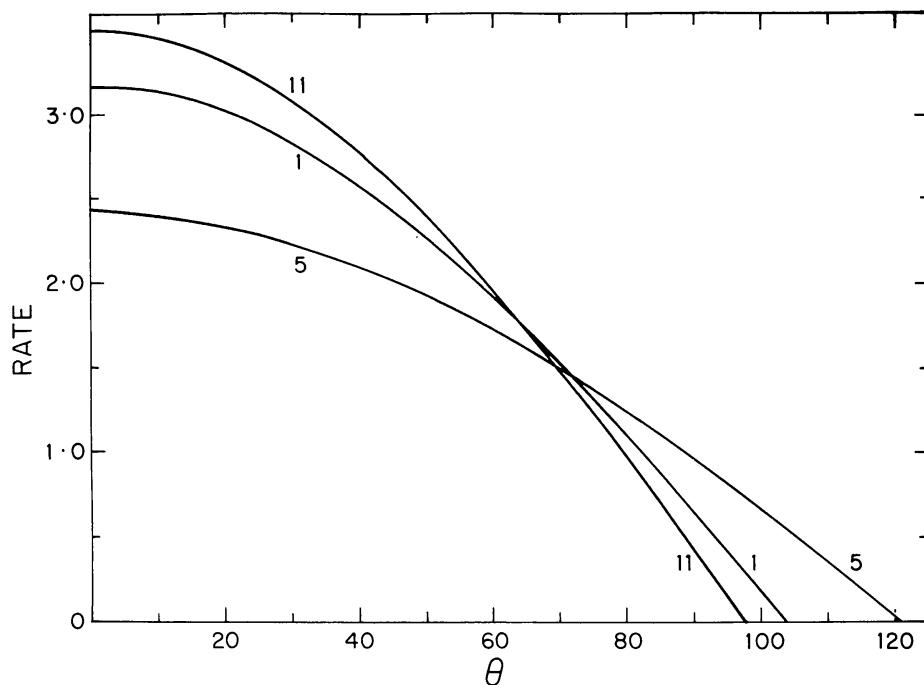


**Fig. 1** Relative rates of meteorite falls as a function of angular distance on the earth from the center of the beam,  $\theta$ , for meteoroids with orbits as listed for entries 1, 5 and 11 in Table 1.

allowed and a contribution of zero is recorded whenever  $\theta$  exceeds the maximum distance over which meteorites could be distributed, i.e.  $\theta$  greater than the intercepts on the abscissa of Figure 1. The arithmetic mean of the 80 values in any cell represents the intensity of meteorite bombardment for that position on the earth in terms of the average over the whole earth taken as unity. A check of the total of these 1146 values showed that a normalizing factor of 1.01 (a 1% correction) should be applied to each value to compensate for slight errors introduced by using discrete intervals to derive the points that were the basis for the curves of Figure 1.

Figure 2 shows the results in the form of a contour map. The hemisphere shown in the figure represents the night side of the earth with the apex-antapex line (the ecliptic) as the diameter from right to left and the north ecliptic pole at the top. The plot is symmetrical about the ecliptic and also about the sunrise-sunset line. To view the daylight side of the earth, turn the figure upside down and interchange labels on the ecliptic poles. To the extent that the choice of orbits in Table 1 represents the population of meteorite-dropping fireballs, Figure 2 is the pattern of relative intensities, fixed with respect to the chosen system of coordinates.

To study the variations of the meteorite fall rate with position and time on the earth we first choose a set of standard geographic latitudes:  $0^\circ$ ,  $13^\circ$ ,  $26^\circ$ ,  $39^\circ$ ,  $52^\circ$ ,  $65^\circ$ ,  $78^\circ$ ,  $90^\circ$ . These are sufficient to examine variations with latitude and have the advantage that  $39^\circ$  is a mid-latitude for the Prairie Network observations and  $52^\circ$  is the mid-latitude of the MORP network. We divide the year into 12 parts defined by choosing solar longitudes of  $0^\circ$ ,  $30^\circ$ ,  $60^\circ$ , . . . as the mid-points of the intervals. For each time of year the earth's pole is defined in Figure 2 and a chosen latitude defines the diurnal path as a small circle about the pole. A computer program was used to locate the position in Figure 2 at hourly intervals throughout the day and to identify which of the 1146 cells contained each point. The intensity value for the particular cell was then read out and the 24 values were tabulated for the day for each of the 12 times of year. The whole operation was performed for each of the 8 selected latitudes. The data were plotted as 96 diurnal curves, one for each combination of solar longitude and geographic latitude. Typical examples are shown in Figure 3.

## RESULTS AND DISCUSSION

The pattern of meteorite distribution shown in Figure 2 has several features of interest. Low values near the apex and high values near the antapex are expected from the direct, low-inclination orbits of Table 1. In fact, the peak intensities near the antapex are drawn out surprisingly far along the ecliptic, so that the values  $90^\circ$  away from the antapex, at the sub-solar and anti-solar points, are only 12% lower than at the antapex. The highest value is not even at the antapex, but shifted  $45^\circ$  along the ecliptic to either side, where the calculated flux is 1% higher than at the antapex.

The rates at the antapex and apex are in the ratio 11:1 (1.44 at the antapex and only 0.13 at the apex). The lack of a prominent peak near the antapex may be contrary to expectation because it is natural to think of the intersecting orbits of meteoroid and the earth in a heliocentric frame whereas it is the geocentric path that determines the direction of arrival and governs the distribution over the earth. Consider, for example, meteor number 12 in Table 1. Its orbit is approximately tangent to the earth's orbit near 1 AU and it is the sort of meteorite presumed to arrive from the antapex direction with a strong preference for arrival near 18<sup>h</sup> local time. In fact, its geocentric radiant is  $29^\circ$  from the

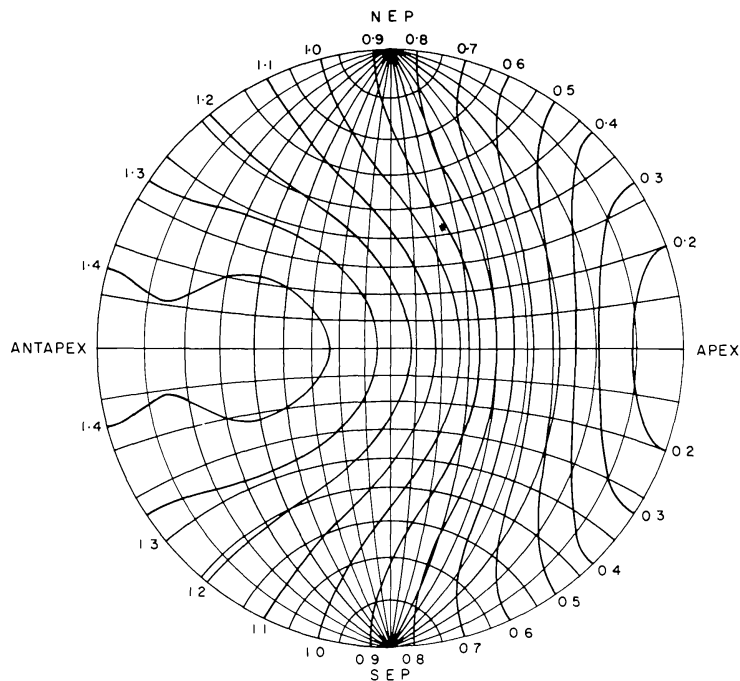


**Fig. 2** Stereographic projection of the night hemisphere of the earth with  $10^\circ$  grid circles. The labels indicate points on the earth facing the apex, antapex, north ecliptic pole (N.E.P.) and south ecliptic pole (S.E.P.). The contour lines indicate the relative rates of meteorite falls from values of 0.2 near the apex to 1.4. For the daytime hemisphere, interchange labels on the north and south ecliptic poles and invert the figure.

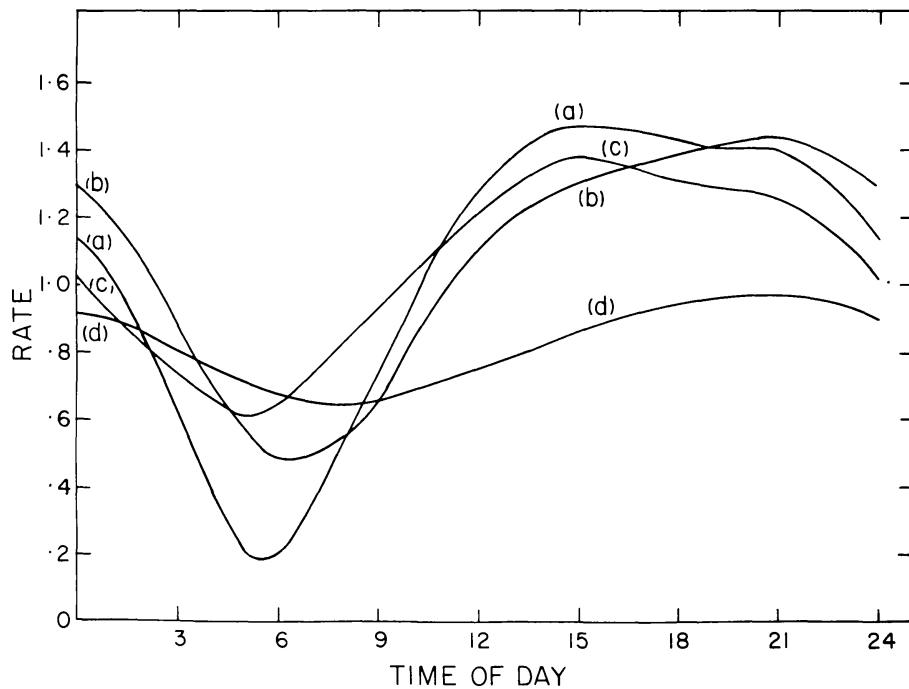


**Fig. 3** Plots of the meteorite fall rate as a function of time of day for some typical cases. (a) latitude,  $\phi = 13^\circ$ , solar longitude,  $\lambda = 90^\circ$ ; (b)  $\phi = 39^\circ$ ,  $\lambda = 300^\circ$ ; (c)  $\phi = 52^\circ$ ,  $\lambda = 60^\circ$ ; (d)  $\phi = 78^\circ$ ,  $\lambda = 240^\circ$ .

antapex and the only area on the earth in which meteorites from its four configurations are excluded is an area bounded by four intersecting small circles, which approximates a cap of radius  $30^\circ$  about the apex and represents less than 7% of the area of the sphere. In a heliocentric view, this object approaches the earth very nearly from the antapex direction, but in a geocentric system with gravitational focusing included, very little of the earth is shielded from its arrival and there is no strong preference for the antapex or 18<sup>h</sup> local time.

Figure 2 shows that the rate of meteorite falls for points beneath the ecliptic poles is about 0.86 of the average value over the earth. This relatively high value again shows the importance of moderate inclinations and gravitational effects. Note that these rates are all *per unit solid angle*; the total number of radiants with  $\theta$  within an increment  $\epsilon$  of  $90^\circ$  is more than four times the number with  $\theta$  within  $\epsilon$  of  $10^\circ$ , due to the larger area of sky involved. In the earlier study (Halliday, 1964) in which all inclinations were taken to be zero, the velocity mixture of the present Table 1 would give a mean value of about 0.64 at the ecliptic pole, due to gravitational focusing alone. The moderate inclinations in Table 1 increase this rate to 0.86 of the normal rate.

How sensitive are the contours in Figure 2 to the particular choice of orbits in Table 1? This may be assessed by examination of the 80 individual components of any of the 1146 cells and observing what change might be caused by removing one (or more) of the entries in Table 1 and replacing it by a different orbit. Near the antapex the totals are quite insensitive to any reasonable change in the makeup of Table 1. At the apex, on the other hand, the major portion of the value depends on the contributions of 5 of the 20 entries in Table 1, the five entries for which the geocentric radiant is more than  $85^\circ$  from the antapex. The largest of these values is  $90.1^\circ$  from the antapex, so even the large contributions to the fall rate at the apex come from values of  $\theta$  in Figure 1 near  $90^\circ$  or larger. It could be argued that: (1) Table 1 should include one or two Aten-type orbits; (2) it already contains too many velocities between 20 and  $23 \text{ km s}^{-1}$  in relation to the expected rate of survival of meteorites from fireballs of this velocity; (3) it should contain one or two entries of even higher velocity, or; (4) it should have a higher concentration of perihelia just inside the earth's orbit. Suppositions (1) and (3) would add significantly to the rates near the apex but (2) implies these rates may be too high as they are. Number (4) would shift some patterns from Figure 1 closer to the antapex and broaden the patterns at the same time, due to a decreased velocity, which would have little effect on the final contours. The net effect of whatever deficiencies of these types exist in Table 1 will be quite small near the antapex but could alter the contour levels close to the apex by as much as a factor of 2.

Table 2 lists, for seven latitudes, the relative rates of meteorite falls for eight times of day and twelve times of year. It is a condensed and partially smoothed version of the data from which the curves of Figure 3 were plotted, where each horizontal line in the table corresponds to a curve of the type in Figure 3. The individual points from which the curves were drawn are the values from one of the 1146 cells and these values frequently change by a few percent of the mean rate between adjacent cells. Where a diurnal path in Figure 2 might run near the edge of a few cells, the central values are still recorded and the plot may then depart systematically from the ideal values, which can show as an occasional lack of smoothness when the values in Table 2 are examined in columns instead of rows. The table and the curves may be used to study variations in the rate as a function of several parameters. For southern latitudes, enter the first column of Table 2 with  $(\lambda + 180^\circ)$  instead of  $\lambda$ .

**Table 2**  
**Diurnal variation in rates for different seasons and latitudes**

Solar long. $\lambda$	Latitude 0°							
	0h	3h	6h	9h	12h	15h	18h	21h
0	1.27	0.74	0.29	0.75	1.29	1.44	1.37	1.44
30	1.28	0.76	0.28	0.71	1.23	1.40	1.38	1.46
60	1.28	0.70	0.25	0.66	1.19	1.40	1.39	1.46
90	1.23	0.66	0.23	0.67	1.23	1.43	1.42	1.43
120	1.19	0.64	0.23	0.72	1.27	1.46	1.40	1.40
150	1.23	0.69	0.25	0.74	1.29	1.46	1.40	1.40
180	1.26	0.76	0.26	0.73	1.27	1.44	1.39	1.44
210	1.28	0.74	0.26	0.71	1.23	1.39	1.40	1.46
240	1.28	0.71	0.24	0.63	1.18	1.39	1.41	1.46
270	1.24	0.66	0.26	0.65	1.23	1.43	1.42	1.43
300	1.19	0.63	0.26	0.71	1.26	1.46	1.39	1.40
330	1.23	0.72	0.28	0.77	1.28	1.46	1.37	1.40
	Latitude 13°							
0	1.29	0.78	0.38	0.77	1.27	1.46	1.40	1.46
30	1.29	0.78	0.32	0.83	1.27	1.46	1.41	1.46
60	1.23	0.68	0.28	0.74	1.24	1.46	1.43	1.44
90	1.13	0.62	0.19	0.73	1.27	1.46	1.42	1.39
120	1.14	0.55	0.18	0.74	1.28	1.46	1.38	1.32
150	1.14	0.63	0.17	0.75	1.27	1.41	1.35	1.33
180	1.20	0.72	0.25	0.71	1.20	1.38	1.34	1.38
210	1.27	0.74	0.21	0.62	1.14	1.32	1.34	1.41
240	1.28	0.74	0.21	0.55	1.12	1.32	1.37	1.46
270	1.28	0.72	0.21	0.61	1.14	1.39	1.43	1.46
300	1.24	0.77	0.30	0.69	1.23	1.44	1.43	1.46
330	1.27	0.83	0.33	0.79	1.28	1.46	1.41	1.46
	Latitude 26°							
0	1.29	0.83	0.51	0.83	1.29	1.46	1.43	1.46
30	1.24	0.78	0.43	0.84	1.29	1.46	1.43	1.44
60	1.15	0.68	0.37	0.88	1.28	1.46	1.41	1.38
90	1.04	0.59	0.27	0.80	1.27	1.45	1.37	1.31
120	1.04	0.50	0.23	0.82	1.24	1.45	1.31	1.22
150	1.03	0.55	0.28	0.73	1.20	1.34	1.32	1.21
180	1.10	0.64	0.22	0.63	1.14	1.24	1.24	1.25
210	1.20	0.74	0.22	0.55	1.04	1.21	1.27	1.33
240	1.27	0.83	0.21	0.50	0.99	1.23	1.33	1.40
270	1.27	0.84	0.26	0.59	1.06	1.31	1.38	1.45
300	1.27	0.88	0.37	0.66	1.13	1.37	1.42	1.46
330	1.29	0.85	0.49	0.79	1.24	1.44	1.43	1.46

Table 2 (continued)

Solar long. $\lambda$	Latitude 39°							
	0h	3h	6h	9h	12h	15h	18h	21h
0	1.24	0.89	0.59	0.89	1.25	1.36	1.36	1.41
30	1.20	0.82	0.56	0.92	1.28	1.43	1.40	1.38
60	1.11	0.64	0.47	0.85	1.28	1.44	1.37	1.30
90	0.96	0.54	0.39	0.88	1.24	1.40	1.34	1.21
120	0.90	0.44	0.29	0.76	1.19	1.34	1.26	1.13
150	0.94	0.50	0.23	0.69	1.12	1.24	1.16	1.08
180	1.03	0.58	0.18	0.58	1.03	1.11	1.15	1.11
210	1.14	0.68	0.24	0.51	0.93	1.07	1.16	1.24
240	1.19	0.75	0.32	0.46	0.86	1.13	1.26	1.34
270	1.24	0.87	0.43	0.54	0.96	1.22	1.34	1.40
300	1.28	0.85	0.48	0.66	1.09	1.30	1.37	1.44
330	1.29	0.89	0.56	0.83	1.20	1.38	1.41	1.43
Solar long. $\lambda$	Latitude 52°							
	0h	3h	6h	9h	12h	15h	18h	21h
0	1.20	0.90	0.72	0.89	1.22	1.34	1.36	1.35
30	1.13	0.83	0.67	0.95	1.23	1.35	1.34	1.30
60	1.02	0.73	0.63	0.92	1.23	1.37	1.30	1.24
90	0.90	0.58	0.54	0.89	1.18	1.29	1.25	1.15
120	0.76	0.48	0.43	0.81	1.13	1.25	1.13	1.04
150	0.79	0.43	0.33	0.65	1.01	1.11	1.04	0.96
180	0.88	0.55	0.27	0.55	0.91	1.02	1.02	1.02
210	1.03	0.65	0.33	0.43	0.79	0.95	1.04	1.10
240	1.14	0.81	0.43	0.48	0.76	1.04	1.12	1.24
270	1.19	0.88	0.54	0.60	0.89	1.14	1.27	1.29
300	1.23	0.92	0.64	0.74	1.02	1.24	1.30	1.37
330	1.24	0.94	0.68	0.83	1.15	1.30	1.34	1.35
Solar long. $\lambda$	Latitude 65°							
	0h	3h	6h	9h	12h	15h	18h	21h
0	1.17	0.96	0.85	0.96	1.17	1.25	1.30	1.25
30	1.08	0.92	0.79	0.96	1.19	1.27	1.27	1.20
60	1.04	0.85	0.78	0.97	1.14	1.29	1.27	1.16
90	0.92	0.70	0.66	0.89	1.12	1.21	1.17	1.05
120	0.73	0.55	0.55	0.82	1.04	1.09	1.06	0.92
150	0.71	0.47	0.43	0.64	0.87	0.96	0.92	0.86
180	0.74	0.49	0.36	0.51	0.76	0.84	0.90	0.83
210	0.93	0.64	0.43	0.47	0.71	0.85	0.92	0.96
240	1.04	0.81	0.55	0.56	0.75	0.96	1.06	1.09
270	1.13	0.88	0.66	0.69	0.86	1.05	1.17	1.20
300	1.15	0.97	0.77	0.84	1.04	1.15	1.26	1.28
330	1.20	0.96	0.80	0.92	1.07	1.20	1.27	1.27

**Table 2 (continued)**

Solar long. $\lambda$	Latitude 78°							
	0h	3h	6h	9h	12h	15h	18h	21h
0	1.10	1.04	0.99	1.03	1.12	1.16	1.20	1.16
30	1.10	1.01	0.97	1.02	1.12	1.18	1.20	1.17
60	0.98	0.91	0.89	0.97	1.09	1.16	1.13	1.10
90	0.86	0.80	0.79	0.92	1.00	1.07	1.06	0.96
120	0.73	0.65	0.67	0.79	0.92	0.96	0.94	0.85
150	0.66	0.58	0.54	0.62	0.72	0.81	0.80	0.75
180	0.60	0.55	0.54	0.54	0.60	0.71	0.80	0.71
210	0.71	0.63	0.54	0.57	0.66	0.76	0.81	0.79
240	0.90	0.79	0.67	0.64	0.74	0.84	0.94	0.96
270	1.00	0.92	0.80	0.80	0.88	0.97	1.05	1.07
300	1.11	0.98	0.90	0.91	0.99	1.09	1.13	1.14
330	1.12	1.01	0.97	1.01	1.09	1.17	1.20	1.16

*Daylight:twilight:night variation*

Due to the effects of atmospheric refraction and semi-diameter of the sun, the area of earth in daylight is that area for which the sun's position is within  $90^{\circ} 51'4''$  of the zenith. We choose nautical twilight or a solar zenith distance of  $102^{\circ}$  as the boundary between twilight and night. For each of the 96 curves of the type in Figure 3, the times of daylight and twilight were determined and the curves integrated for the relative numbers of falls during the three conditions of illumination. Weighting each zone of latitude in proportion to the corresponding area on the earth we obtain the comparison in Table 3 which shows the division of the earth and of meteorite falls among the three zones. The ratios of meteorite falls to areas give the average relative rates, shown in the final column.

Although evening twilight invariably has a high rate in Figure 3, it is more than offset by the low rates in morning twilight. As shown in Table 3, the average value for twilight is relatively poor and the night values are actually highest. Camera networks are thus not at a disadvantage as far as meteorite fall rates are concerned, contrary to some previous conclusions.

**Table 3**  
**Falls during daylight, twilight and night**

	Proportion of earth's area	Proportion of falls	Relative Rate
Daylight	0.508	0.508	1.00
Twilight	0.096	0.082	0.85
Night	0.396	0.410	1.03

### *Time of day variations*

The data in Table 2 may be averaged throughout the year to determine the variation of the fall rate during the day for a particular latitude. Figure 4 shows four of the curves for a range of latitudes and also a mean curve averaged over all latitudes, again weighted by their relative areas.

The curves show an approximately level rate between noon and midnight and have a pronounced dip at 6 a.m. The minimum becomes less pronounced with increasing latitude (north or south) and of course disappears at the poles. The 6 a.m. minimum is a direct consequence of the low values near the apex in Figure 2 and the depth of the minimum would be sensitive to the addition or removal of a few high-velocity meteorites in the sample, as discussed previously. The variation in rates between 6 a.m. and the afternoon maximum is considerably greater than for Wood's (1961) theoretical curves (his figure 11) probably due to the uncorrected effects of error dispersion in the old visual data.

Wetherill (1968) has studied the time-of-day distribution to be expected from different possible sources for meteorites, after the initial orbits have evolved for periods comparable to the cosmic-ray exposure ages of stone meteorites. He found that initial orbits of low inclination with perihelia just within the earth's orbit and aphelia near 4.5 AU were the only ones to give a reasonable match to the observed afternoon to morning excess of meteorite falls. More recently (Wetherill, 1979) he has investigated the populations of Apollo-Amor objects to be expected from different initial sources and found the cometary component is likely to dominate over the asteroidal component. Wetherill (1968) quotes 0.66 as the observed value for the fraction of "daytime" meteorites (falls between 0600 and 1800 hours) which fell after noon. From the mean curve in our Figure 4 we derive 0.62 for this value and note that the small difference may be explained by a greater efficiency of recovery in the afternoon. Farmers are more likely

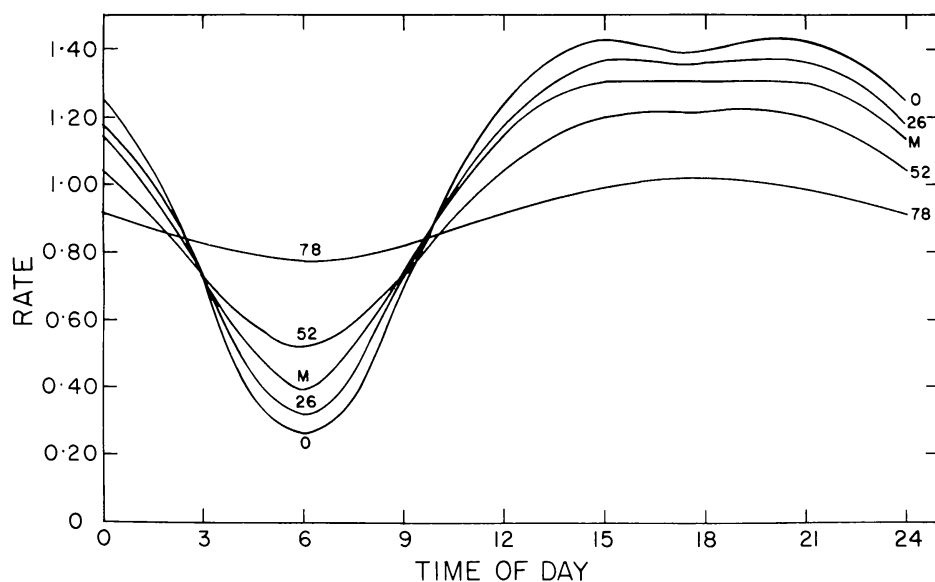


**Fig. 4** Mean values for the year at each hour of the day for latitudes of  $0^\circ$ ,  $26^\circ$ ,  $52^\circ$ ,  $78^\circ$  and the weighted mean for the whole earth, labeled M.

to be on the land between 1600 and 1800 than between 0600 and 0800 local time, because of the tendency to perform indoor chores in the early morning while crops are wet from dew.

Our results indicate an afternoon excess of meteorite falls for any distribution of fireballs limited at the high-velocity end by some limit beyond which the atmosphere acts as a severe filter. If the achondrites do have a morning excess, as possibly suggested by the observational data in Wetherill's (1968) figure 1B, then this implies elongations from the antapex in excess of  $90^\circ$  and pre-atmospheric velocities generally in the range from 25 to  $35 \text{ km s}^{-1}$  (or else a surprisingly large component of Aten-type orbits). Some meteorites may survive such encounters and if the achondrites presently reaching the earth are fragments of one or a very few objects with orbits that produce encounter velocities in this range, then the morning excess may be quite valid.

### Seasonal variations

The seasonal variation in rates is derived by plotting, for each latitude, the daily mean rates derived by integrating the curves of Figure 3, as a function of solar longitude. The data are listed in Table 4 and Figure 5 is a selection of the seasonal plots, for the same latitudes as in Figure 4 and also for the average over the hemisphere. The figure represents data for the northern hemisphere only, where  $0^\circ$  solar longitude is the beginning of spring. For southern latitudes shift the scale of solar longitude by  $180^\circ$  and the curves are then correct, i.e. maximum values occur near the beginning of spring in both hemispheres.

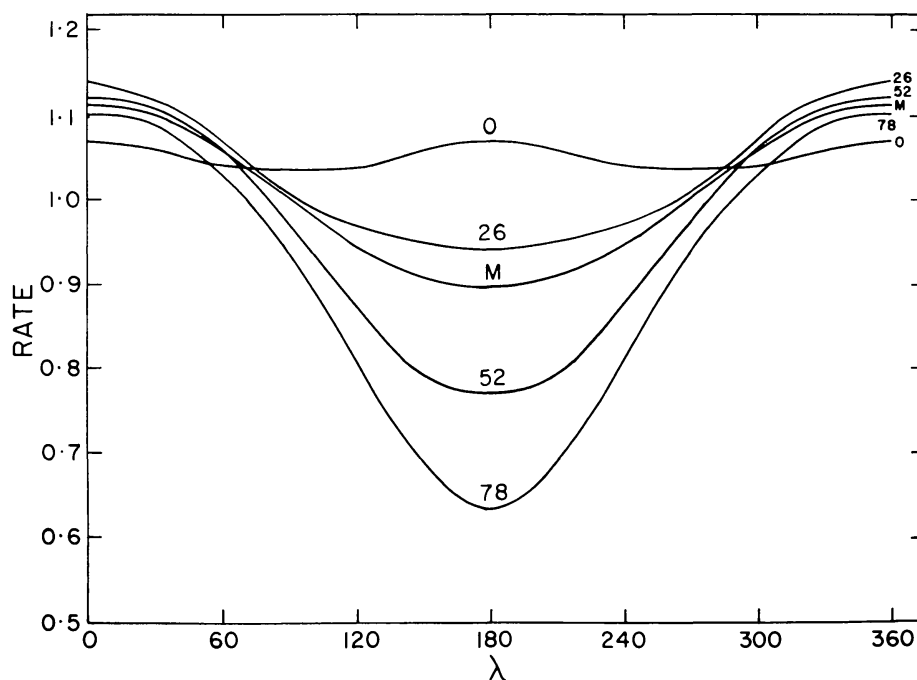


**Fig. 5** The variation in rates with season (solar longitude,  $\lambda$ ) for latitudes of  $0^\circ$ ,  $26^\circ$ ,  $52^\circ$ ,  $78^\circ$  and the mean curve, M, for one hemisphere (north is shown). For southern latitudes, shift the scale of  $\lambda$  by  $180^\circ$ .

**Table 4**  
**Daily average rates for different seasons and latitudes**

Solar long. $\lambda$	Geographic latitude							
	0°	13°	26°	39°	52°	65°	78°	90°
0	1.07	1.11	1.14	1.13	1.12	1.11	1.10	1.11
30	1.06	1.10	1.12	1.12	1.11	1.09	1.09	1.09
60	1.04	1.06	1.07	1.06	1.06	1.06	1.03	1.02
90	1.04	1.03	1.01	1.00	0.97	0.96	0.94	0.91
120	1.04	1.01	0.97	0.92	0.88	0.85	0.81	0.79
150	1.06	1.01	0.95	0.87	0.79	0.74	0.69	0.68
180	1.07	1.02	0.94	0.85	0.77	0.69	0.63	0.65
210	1.06	1.01	0.95	0.87	0.79	0.74	0.69	0.68
240	1.04	1.01	0.97	0.92	0.88	0.85	0.81	0.79
270	1.04	1.03	1.01	1.00	0.97	0.96	0.94	0.91
300	1.04	1.06	1.07	1.06	1.06	1.06	1.03	1.02
330	1.06	1.10	1.12	1.12	1.11	1.09	1.09	1.09
Average	1.052	1.046	1.027	0.993	0.959	0.933	0.904	0.895

The seasonal variation is quite appreciable for latitudes outside the tropics. Maximum values lie between 1.10 and 1.14 of normal, except near the equator, but the minima have a wide range, dipping below 0.7 near the autumnal equinox at high latitudes. The diurnal path in Figure 2 is then essentially confined to the upper portion of the upper-right quadrant of the figure. The minima in Figure 5 are less sensitive to the values close to the apex than are the deeper minima in Figure 4, due to the nature of the averaging in the two cases.

An interesting feature of the seasonal variation is the change in the rate of meteorite falls between the two seasons of maximum agricultural activity. For many latitudes the rate is more than 30% higher during spring planting operations than during the harvest season. Although rates are higher in winter than in summer, it may be that winter recovery rates suffer from short hours of daylight and fewer people in a position to respond as witnesses. On the other hand, when winter conditions are severe enough to provide ice surfaces, frozen soil and at least some snow cover, they may improve chances of recovery as indicated by a brief survey of witnessed falls in Canada (Halliday *et al.*, 1978, p. 35).

#### *Latitude variation*

If the data in Table 4 are examined as a function of latitude instead of solar longitude, then a moderate dependence on geographic latitude is observed. Mean values for the year are shown at the bottom of each column and these vary from 1.05 at the equator to 0.89 at the geographic poles. Note that the polar value is slightly higher than the value of 0.86 for the ecliptic pole from Figure 2.

## CAMERA NETWORKS AND RATES OF METEORITE FALLS

Table 3 shows that meteorite arrival rates average 1.03 of normal during hours of darkness and this factor is essentially independent of latitude. With mean latitudes of  $39^\circ$  and  $52^\circ$  for the Prairie Network and MORP camera network, the average rates are 0.99 and 0.96 for the whole year or 1.02 and 0.99 for the mean nighttime rates for the PN and MORP networks. Either network thus observes directly what is essentially the average rate of meteorite falls on the entire earth (since the statistics of which events are true observed falls will be uncertain by much more than 2%) and it appears there was no need for the correction factor of 2, assumed by McCrosky and Ceplecha (1969, p. 604). An estimate of the number of meteorites arriving per  $10^6$  km<sup>2</sup> per year on the basis of observations by the MORP network will be the subject of another paper. The observed rates will require a correction of only 1% to allow for the average rate of 0.99 found above for latitude  $52^\circ$  at night. The European Network is intermediate in latitude between the PN and MORP networks and will have very similar rates.

It is of interest to examine the relative rates of falls predicted from this paper for the actual times of fall of the three meteorites photographed by camera networks. Using the appropriate local times of fall, the relative rates are 1.32 for Pribram, 1.41 for Lost City and 1.37 for Innisfree. All three are quite high values, in accord with the fact that all fell during the evening and within 0.2 year from the vernal equinox.

### SUMMARY

The significant results of this study may be summarized as follows:

1. Gravitational focusing near the earth is important. As a result, typical meteorite orbits may lead to meteorite falls at almost any point on earth.
2. Meteorite fall rates at any moment are highest in a broad area near the antapex of the earth's motion. Although the heliocentric orbits have a strong concentration of arrival directions near the antapex, in a geocentric system there is no sharp peak.
3. There is a deep minimum in rates near the apex, the magnitude of which is sensitive to the velocity cutoff by the atmosphere for fast meteorites.
4. The ratio of the rate near the antapex to that near the apex is estimated as 11 to 1.
5. Twilight rates are lower than average due to the influence of the area near the apex. Mean rates of meteorite falls at night are 3% higher than during daylight.
6. Fall rates are approximately constant from noon to midnight and there is a minimum near 6 a.m. The depth of the minimum decreases for higher geographic latitude. For meteorite falls between 0600 and 1800 hours (daylight falls) the model predicts 62% will fall after noon, in good agreement with the observed ratio of afternoon to morning falls.
7. Meteorite rates are highest near the beginning of spring in either hemisphere and lowest at the beginning of autumn. Outside the tropics the variation is about 30%.
8. There is only a modest decline in the meteorite rate with increasing latitude. The value at the pole is 85% of the equatorial value.
9. The nighttime rates for the meteorite camera networks in Europe and North America are within 2% of the mean rates for the whole earth.

## REFERENCES

- Ceplecha, Z.**, 1977. Fireballs photographed in central Europe. *Bull. Astron. Inst. Czechoslovakia* **28**, 328-340.
- Ceplecha, Z. and R.E. McCrosky**, 1976. Fireball end heights: a diagnostic for the structure of meteoric material. *Jour. Geophys. Res.* **81**, 6257-6275.
- Halliday, I.**, 1964. The variation in the frequency of meteorite impact with geographic latitude. *Meteoritics* **2**, 271-278.
- Halliday, I.**, 1973. Photographic fireball networks. In *Evolutionary and Physical Properties of Meteoroids*, C.L. Hemenway, P.M. Millman and A.F. Cook, ed. NASA SP-319, Washington, 1-8.
- Halliday, I., A.T. Blackwell and A.A. Griffin**, 1978. The Innisfree meteorite and the Canadian camera network. *Jour. Roy. Astron. Soc. Canada* **72**, 15-39.
- Levin, B. Ju. and A.N. Simonenko**, 1969. Meteorite radiants and orbits. In *Meteorite Research*, P.M. Millman, ed. D. Reidel Pub. Co., Dordrecht, Holland, 552-558.
- McCrosky, R.E. and Z. Ceplecha**, 1969. Photographic networks for fireballs. In *Meteorite Research*, P.M. Millman, ed. D. Reidel Pub. Co., Dordrecht, Holland, 600-612.
- Millman, P.M.**, 1969. Astronomical information on meteorite orbits. In *Meteorite Research*, P.M. Millman, ed. D. Reidel Pub. Co., Dordrecht, Holland, 541-551.
- Misconi, N.Y.**, 1980. The symmetry plane of the zodiacal cloud near 1 AU. In *Solid Particles in the Solar System*, I. Halliday and B.A. McIntosh, ed. D. Reidel Pub. Co., Dordrecht, Holland, 49-53.
- ReVelle, D.O.**, 1979. A quasi-simple ablation model for large meteorite entry: theory vs. observations. *Jour. Atmospher. Terrestr. Phys.* **41**, 453-473.
- Simonenko, A.N.**, 1975. Orbital elements of 45 meteorites. Atlas. U.S.S.R. Academy of Sciences, Committee on Meteorites Moscow. 68 pages, in Russian.
- van de Kamp, P.**, 1960. Elements of astromechanics. *Jour. Roy. Astron. Soc. Canada* **60**, 1-11, 69-78, 110-125, 167-176, 231-244, 275-283.
- Wetherill, G.W.**, 1968. Time of fall and origin of stone meteorites. *Science* **159**, 79-82.
- Wetherill, G.W.**, 1979. Steady state populations of Apollo-Amor objects. *Icarus* **37**, 96-112.
- Wood, J.A.**, 1961. Stony meteorite orbits. *Monthly Notices Roy. Astron. Soc.* **122**, 79-88.

Manuscript received 6/18/81